Polystyrene Foams. I. Processing-Structure Relationships

Saeed Doroudiani*, Mark T. Kortschot

Department of Chemical Engineering and Applied Chemistry, University of Toronto, Toronto, Ontario, Canada M5S 3E5

Received 21 June 2002; accepted 11 February 2003

ABSTRACT: In this study, processing-structure relationships in expanded polystyrene (EPS) made using near-critical carbon dioxide as a physical blowing agent were investigated. In order to investigate the relationship between structure and properties of EPS it was necessary to be able to make samples with a wide range of controlled structures. For this reason, a systematic investigation of the relationship between processing conditions and structure was performed based on a statistical experimental design. Regression analysis was conducted on the data and expressions were developed to quantify the relationships between structural parameters and processing conditions. The samples were saturated with carbon dioxide at relatively high pressure and ambient temperature and the saturated specimens were expanded at elevated temperatures. The importance of the individual processing parameters was determined. Statistical analysis of data showed that foaming time was the most important factor determining foam density, whereas saturation pressure was the most important factor determining cell size and cell density. By controlling the foaming conditions, EPS samples having the same densities and different cell sizes were produced. © 2003 Wiley Periodicals, Inc. J Appl Polym Sci 90: 1412–1420, 2003

Key words: foam; polystyrene; microstructure; microcellular

INTRODUCTION

In the last century polymer foams have been a large and important category of industrial plastics. Polymer foams can be used in many applications, such as insulation, packaging, structures, and filters.[1] Several remarkable properties have been noted for microcellular foams. Specifically, they can offer good mechanical properties[2,3] and a reduction on material costs and weight at the same time.

Various blowing agents (or foaming agents) are used to produce polymer foams. The selection of the blowing agent mainly depends on the basic material and foaming process. The blowing agents may be divided into two major groups, physical and chemical. The physical blowing agents are usually compressed gases and volatile liquids such as nitrogen, carbon dioxide, hydrocarbons, ketones, and alcohols. Chemical blowing agents are generally solid organic or inorganic materials, which evolve gas by a chemical reaction or decomposition within a temperature range. In many applications, the use of a physical blowing agent is appropriate.

The technique of foaming polymers using physical blowing agents (as opposed to chemical ones) was first used by Pfleummer.[4] He exposed rubber to nitrogen gas under 20.7 MPa pressure and made expanded rubber. Alderson[5] patented a process for producing expanded polyethylene using ethylene as blowing agent. Two decades later Gent and Tompkins[6] published an experimental study of the nucleation and growth of gas bubbles in crosslinked elastomers. Hendrey[7] generated foams by introducing an inert gas into a granular mixture of thermoplastic materials so that the gas was thoroughly intermixed among the granular particles. The gas was then held under pressure (sufficient pressure to assure no gas was expelled during the process), while the granular particles were reduced to a flowable material. The plastic material was then conveyed at a relatively low pressure to an injection assembly and subsequently into the mold cavity. In 1981, this technique was modified by Martini et al.[8] Later Martini-Vvedensky et al.[9] described a batch processing technique involving three steps: saturating the polymer with volatile blowing agent, pressure drop (nucleation of cells), and heating the polymer/gas system (growth of the cells). Arora et al.[10] reported a method for producing controlled PS foam structure by manipulating processing conditions using super critical CO_2 as a foaming agent. The authors produced bimodal structures by decompression of the saturated samples in two steps with two different pressures. Another technique was employed by Sumarno et al.[11] to produce microcellular polystyrene using nitrogen as a blowing agent. In this method, the saturation step was conducted at elevated temperatures, and the decompression and cooling rates were

Correspondence to: M. T. Kortschot (kortsch@chem-eng.utoronto.ca).

*Current address: Department of Chemical Engineering, Kyoto University, Sakyo-ku, Kyoto, 606-8501 Japan.

Journal of Applied Polymer Science, Vol. 90, 1412–1420 (2003)

used as controlling tools to obtain the desired structure.

In the last decade, the term "microcellular plastics" has been used to describe all foams made using physical blowing agents in a batch process; however, this process does not always lead to small cell sizes. In general, when the cell size is less than 10 μm, the foams are usually referred to as microcellular foams.

At present, various techniques are used to produce microcellular polymers.[12] These include physical phase separation techniques (thermally induced phase separation),[13–15] precipitation with a liquid anti-solvent,[16–18] spray drying,[19] compositional quenching[20] and rapid expansion from supercritical solution,[11,21–23] or chemical reaction.[24,25] These techniques are usually performed in a batch process. Expanded polymers have also been produced in semicontinuous[26,27] and continuous processes.[28–35]

In order to investigate the relationship between structure and properties of expanded polystyrene (EPS) it was necessary to be able to make samples with a wide range of controlled structures. For this reason, a systematic investigation was performed based on a statistical experimental design. Various processing conditions were used and the structures of the resulting foams were examined using a scanning electron microscope (SEM). Regression analysis was conducted on the data and expressions were developed to quantify the relationship between structural parameters and processing conditions. Moreover, the importance of the individual processing parameters was determined using a statistical analysis of data.

MATERIALS AND METHODS

Materials and sample preparation

The material employed in this study was polystyrene (Novacor PS 2282), with a density of 1040 kg/m^3 and melt index of 11 dg/min (ASTM D-1238). The PS resin was supplied by NOVA Chemicals Company (Calgary, Canada). Clear sheet specimens of PS were made by compression-molding the raw materials to a uniform thickness of 1 mm in a hydraulic hot press (Wabash Metal Products Inc., Model 50-1818-2 TM). The compression-molding temperature was 230°C for about 10 min and the mold was cooled in the press by circulating cold water in the press platens jackets. Rectangular specimens were cut from the PS sheets for foaming process.

Foaming process

In this study a three-stage batch foaming process using near critical CO_2 as a blowing agent was utilized. The samples were first saturated in a pressure vessel with CO_2 at room temperature (23–25°C) and pressures of 3, 4.5, and 6 MPa. These conditions are near the critical point of CO_2, which is at $T_c = 31.1$°C and $P_c < 7.34$ MPa. The required saturation time was determined from the absorption curves,[36] which was about 20 h. After saturation, the pressure was quickly relieved and the samples were put in a glycerin bath for various periods of time at different temperatures. They were then quenched in cold water to stop foaming and to fix the structure of foamed products. For each foaming conditions at least three specimens were prepared. The specimens were conditioned at room temperature and humidity for at least two weeks before any characterizations and mechanical testing. The foaming conditions and saturation times are described in detail in Table I. The pressure vessel used in the experiment has been described in detail previously.[37] Figure 1 schematically shows the set up for foaming.

Foam characterization

The microstructures of expanded samples were characterized using an SEM (HITACHI, model S-520) at an acceleration voltage of 20 kV. The samples were immersed in liquid nitrogen for 10 min, fractured, and mounted on stubs. The fracture surfaces were sputter coated with gold prior to microscopy. The cell population densities were calculated based on the method suggested by Kumar and Suh.[26] In this method the cell density is determined by dividing the number of cells per unit volume of foam by the volume of unfoamed polymer in a unit volume of foam. The cell density was determined using SEM micrographs and eq. (1):

$$N_c = \left(\frac{nM^2}{A}\right)^{1.5} \left(\frac{\rho_s}{\rho_f}\right) \tag{1}$$

where n, M, A, ρ_s, and ρ_f are the number of cells in the micrograph, the magnification of the micrograph, the area of the micrograph, densities of plain sample and expanded sample, respectively. The density of plain and expanded specimens were determined by the Archimedes water immersion method using a high precision analytical balance and eq. (2):

$$\rho_f = \left(\frac{m_0}{m_0 - m_w}\right)\rho_w \tag{2}$$

where m_0 and m_w are the weight of the specimen in air and immersed in water, respectively, and ρ_w is the density of water. The foam relative density ρ_r is the ratio of the foam density ρ_f and the plain (unfoamed) polymer density ρ_s.

Experimental design

In this set of experiments, the cell size, cell density (the number of cells in a unit volume), and foam density

TABLE I
Processing Conditions and Foam Characteristics for Samples

Pressure (MPa)	Temperature (°C)	Time (sc)	Cell size (μm)	Cell density (cells/cm^3)	Relative density
3	105	10	92	1.88E+07	0.5663
3	105	10	81	2.89E+07	0.5547
3	105	30	163	1.39E+07	0.2414
3	110	20	118	4.35E+07	0.2107
3	120	10	27	3.03E+09	0.2424
3	120	30	341	3.30E+06	0.1275
4.5	105	20	74	1.15E+08	0.2911
4.5	110	10	77	6.80E+07	0.3809
4.5	110	20	112	6.04E+07	0.1836
4.5	110	20	114	6.10E+07	0.1745
4.5	110	30	132	6.73E+07	0.1098
4.5	110	30	148	4.61E+07	0.1133
4.5	120	20	145	4.54E+07	0.1212
4.5	120	20	133	5.53E+07	0.128
6	105	10	3	1.40E+12	0.3361
6	105	30	29	7.44E+09	0.0952
6	110	20	15	5.07E+10	0.1004
6	120	10	23	6.58E+09	0.1927
6	120	30	57	3.14E+09	0.0318

(g/cm^3) of neat EPS produced in a foaming process using CO_2 as a blowing agent were parameters of interest. The variables were saturation pressure, foaming temperature, and foaming time, with three levels for each. The experiment was performed based on a central composite design. Central composite designs are combinations of two-level full or fractional designs and star designs. Star designs are minimum sized designs that consist of the axial points of the corresponding 3^3 full factorial design and the center point.[38] The center point corresponds to the test run in which all variables are set at their middle level. According to Montgomery,[39] a central composite design is an excellent way to obtain an indication of curvature while keeping the size and complexity of the design low. The experimental data obtained from Table I were analyzed using CARD™ computer software in order to determine the key components that had significant effects on the foam structure.

Table I presents the test matrix for the three variables at three levels each. In this design four replicates yielded an estimate of the experimental error. A regression model relating the response Y to variables x_1 (representing saturation pressure), x_2 (representing foaming temperature), and x_3 (representing foaming time) supported by this design is:

$$Y = \beta_0 + \beta_1 x_1 + \beta_2 x_2 + \beta_3 x_3 + \beta_{12} x_1 x_2 + \beta_{13} x_1 x_3 + \beta_{23} x_2 x_3 + \beta_{11} {x_1}^2 + \beta_{22} {x_2}^2 + \beta_{33} {x_3}^2 + \varepsilon$$

Note that Table I is ordered according to the processing conditions, but that the testing order was randomized.

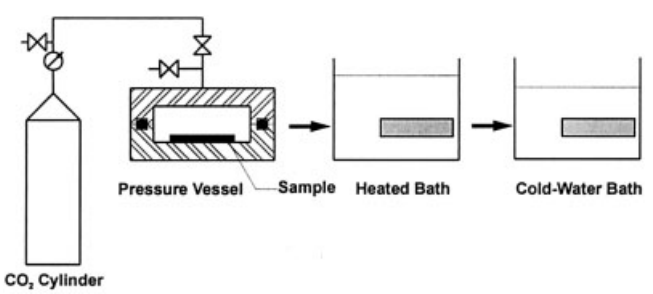

Figure 1 Foaming setup.

RESULTS AND DISCUSSION

The objective of this work was to explore the effects of processing parameters on the structure of EPS in order to make samples with a wide range of controlled structures. After preparing the samples using conditions given in Table I, the expanded samples were fractured in liquid N_2 and their internal structures were examined using SEM. A summary of the experimental results of structures is also given in Table I.

In the foaming process a wide range of foam densities and average cell sizes were obtained. The relation between the cell density (N_0), cell diameter (d), and foam density (ρ_r) is given by simple geometric considerations[40]:

$$\rho_r = \frac{\rho_f}{\rho_s} = \frac{m_f/V_f}{m_s/V_s} = \left(\frac{m_f}{m_s}\right)\left[\frac{V_s}{(V_s + V_g)}\right] = \frac{V_s}{V_s + V_g}$$

Rearranging this equation gives:

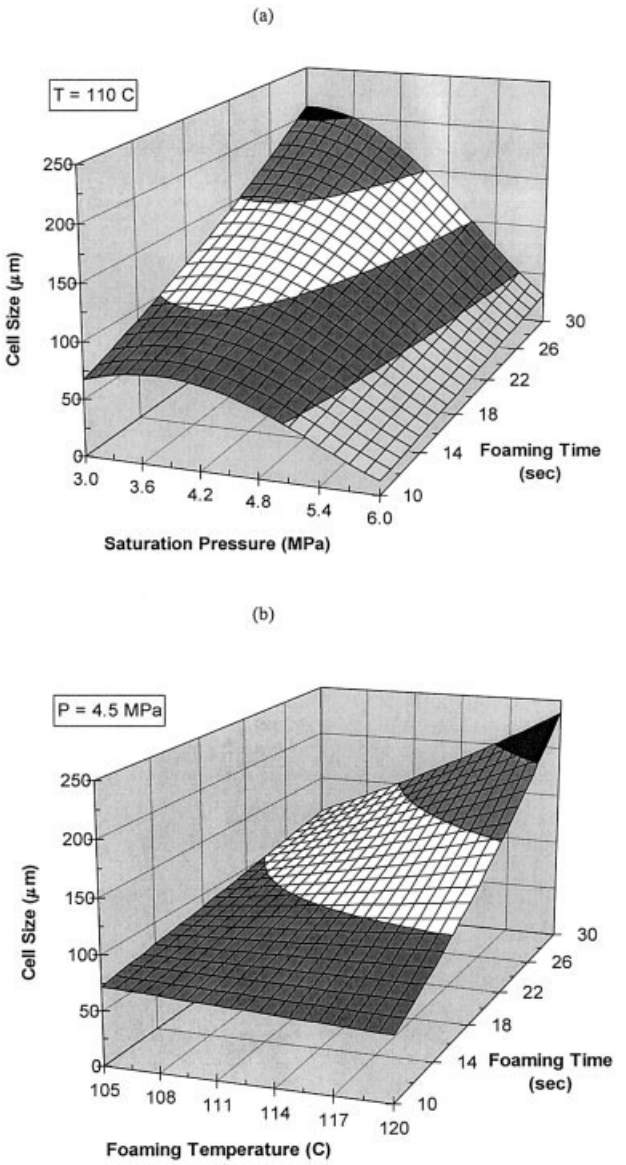

Figure 2 Effect of foaming conditions on the cell size of EPS. The surfaces represent the fitted regression model (eq. 4).

$$\rho_r^{-1} = 1 + V_g/V_s$$

This equation for a unit of volume leads to the following simple expression:

$$N_0 \times \pi d^3/6 = \rho_r^{-1} - 1 \quad (3)$$

Equation (3) indicates that for a given relative foam density (ρ_r), if the cell size (d) increases, then the cell density (N_0) will decrease.

The dependence of cell size, cell density, and foam density on the foaming conditions is shown in plots of Figures 2–4. In this section, using these plots, the effects of saturation pressure, foaming temperature, and foaming time on the foam structure are discussed.

The regression expressions for cell size (d), cell density (N_0), and relative foam density (ρ_r) are presented in eqs. (4), (5), and (6), respectively.

$$\sqrt{d} = 1.204 - 2.309P + 0.132T + 0.247t - 2.368\overline{P}^2 - 1.119\overline{P}\,\overline{t} + 1.369\overline{T}\,\overline{t} \quad (4)$$

$$\mathrm{Log}N_0 = 11.009 + 2.111P - 0.121t + 2.617\overline{P}^2 - 1.267\overline{P}\,\overline{T} \quad (5)$$

$$\rho_r = 1.7791 - 0.0412P - 0.0109T - 0.0109t - 0.03128\overline{P}^2 + 0.0545\overline{T}^2 + 0.0562\overline{t}^2 + 0.0281\overline{P}\,\overline{T} + 0.03815\overline{T}\,\overline{t} \quad (6)$$

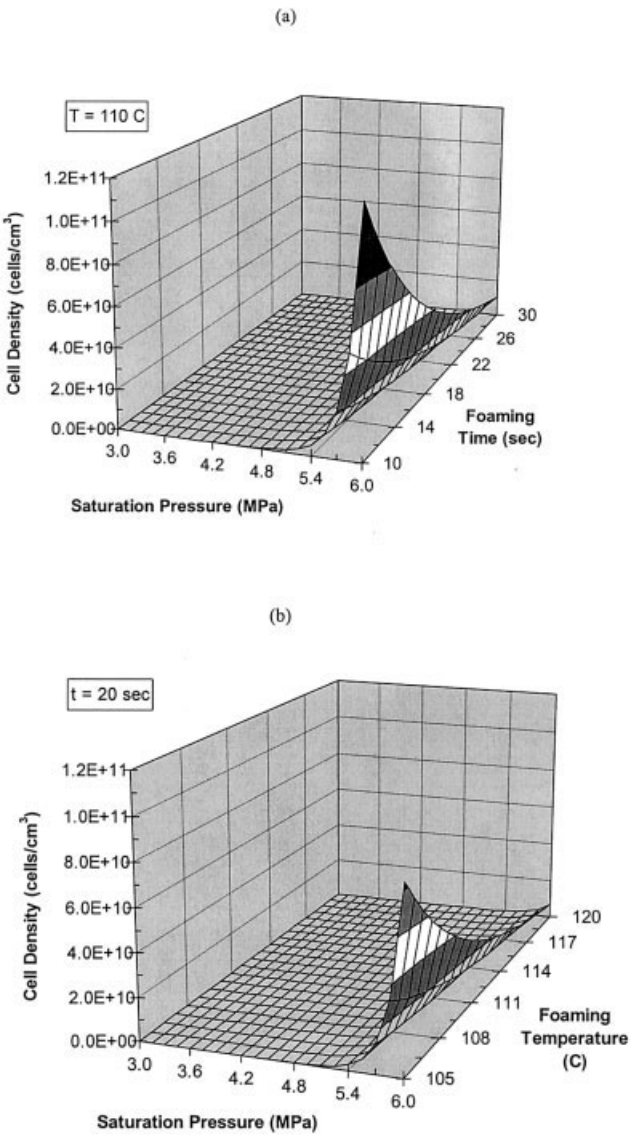

Figure 3 Effect of foaming conditions on the cell density of EPS. The surfaces represent the fitted regression model (eq. 5).

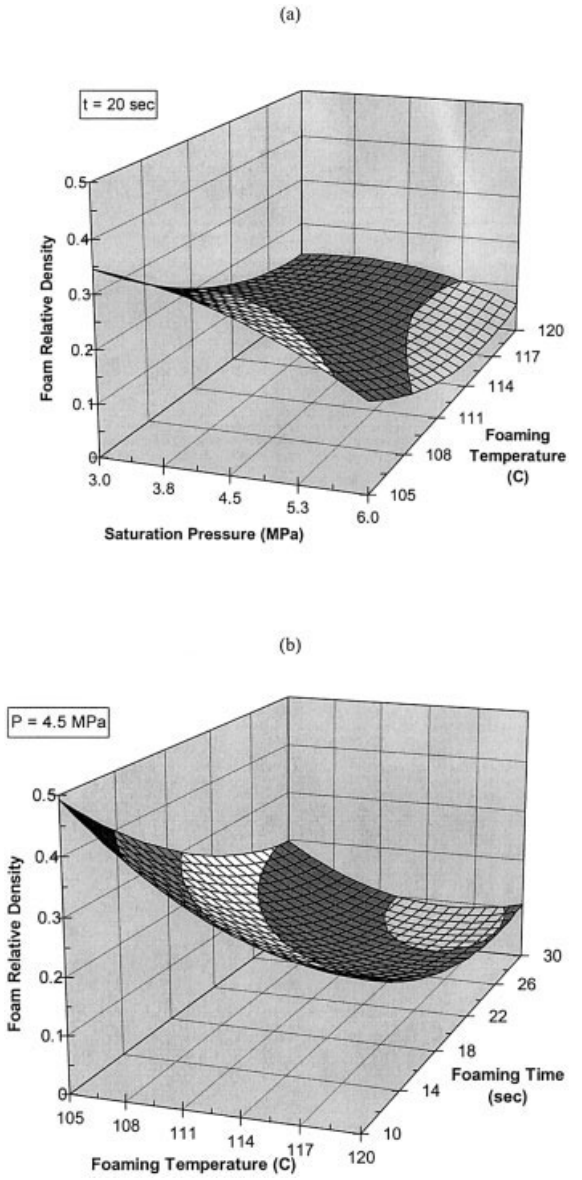

Figure 4 Effect of foaming conditions on the relative density of EPS. The surfaces represent the fitted regression model (eq. 6).

where $\bar{P}=P-4.5/1.5$, $\bar{T}=T-112.5/7.5$, and $\bar{t}=t-20/10$ are scaled (or coded) forms of P, T, and t, respectively. Scaled forms of factors are usually used to arrange the levels of factors. They are made by subtracting the mean of factors from each factor, divided by the distance between the levels. Then the scaled levels appear as -1, 0, and $+1$ in the design matrix, if the two outside levels have the same distance from the mean.

Analysis of the model term effects indicated that saturation pressure (P) was the most important factor determining the cell size and the cell density, followed by foaming time (t) and foaming temperature (T). The term PT, which indicates the interaction between saturation pressure and foaming temperature, was also found to have a significant effect on the cell size and cell density. From an analysis of variance,[37] the model terms ranks for P, t, and T were 1, 0.74, and 0.39, respectively. The model term ranking presents the relative ranking of each model term, which is based on the magnitude of each term's effect on the response relative to that of other terms. The model terms are ranked on a relative scale of 0 to 1, with 1 as the rank of the term with the greatest effect across its experiment range. The analyses were performed in two steps. First, all model terms were considered and statistical parameters were calculated. In the second step, only significant terms (terms with confidence levels of greater than 90%) were considered.

Figure 4 demonstrates the dependence of foam density on the foaming conditions. The foam density decreased with increasing foaming time. Analysis of the model term effects showed that foaming time was the most important factor determining foam density, followed by foaming temperature and saturation pressure. Moreover, the term $T \times t$, which indicates interaction between foaming temperature and foaming time, also had a significant effect on the foam density. While eq. (5) is useful for making design predictions and evaluating the effects of parameters, it does not give detailed physical interpretation of parameters and the mechanisms governed by the process.

Effect of saturation pressure

Scanning electron micrographs of EPS samples produced at low and high levels of CO_2 pressure are shown in Figure 5. The cell density increased from 1.39×10^7 cells/cm^3 to 7.44×10^9 cells/cm^3 as the saturation pressure increased from 3 MPa to 6 MPa, while the average cell size decreased from 163 μm to 29 μm. The resulting foams were closed cell, since the cells were discrete and not connected.

In homogeneous nucleation, cells are formed in the bulk of the liquid, well away from any surface (foreign bodies or the free liquid surface). The nucleation of microcells is a process by which microscopic fluctuations resulting from thermodynamic state changes create clusters of gas molecules. The nucleated clusters will spontaneously grow if they exceed a critical size. Clusters smaller than the critical size will dissolve back into solution. This implies the existence of a finite energy barrier. In homogeneous nucleation this energy (Gibbs free energy) for a bubble with a radius of r can be expressed as a function of pressure of the gas in the bubble (ΔP), and the surface energy of the polymer-bubble interface (γ).[41]

$$\Delta G^* = \left(\frac{16\pi}{3\Delta P^2}\right)\gamma^3 \tag{7}$$

The amount of dissolved CO_2 in the polymer increases from about 5% by weight at 3 MPa to about 8%

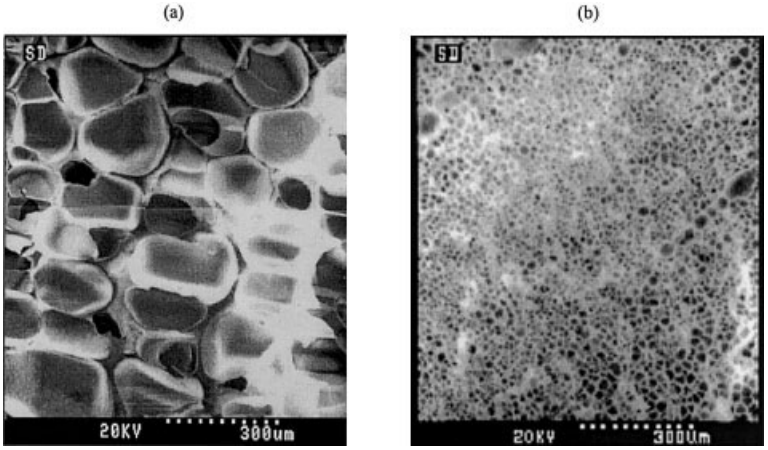

Figure 5 SEM micrographs of the specimens produced at CO_2 saturation pressure (a) 3 MPa and (b) 6 MPa. Foaming temperature and time were set at 105°C and 30 s, respectively.

by weight at 6 MPa, which leads to greater supersaturation. Not surprisingly the level of supersaturation of gas in the polymer has the largest effect on the nucleation of cells. For homogeneous nucleation greater supersaturation produces greater instability than a lower level of supersaturation, which leads to more nucleation sites. In the case of heterogeneous nucleation, in which the nucleation takes place in the presence of foreign bodies such as additive particles, the degree of supersaturation of gas in the polymer and both the number and kind of nucleator particles determine the morphology and cell size of the resultant foam. Heterogeneous nucleation generally results in a higher number of cells, provided there is an abundance of nucleation sites.

Compressed fluids, like CO_2, dissolve in PS and depress its glass transition temperature (T_g) significantly. While this phenomenon may have affected the foaming process of PS, it has been reported elsewhere.[36] It has been shown that[42] a compressed fluid with a low solubility will act strictly as a pressure-generating medium, thus increasing the T_g with increasing pressure. While a more soluble fluid can effectively plasticize a polymer and decrease T_g, the higher levels of dissolution of compressed fluid in the polymer cause a greater depression in T_g. Models have been proposed to predict the T_g depression of a polymer caused by dissolution of a compressed fluid for various systems. Sorption of CO_2 in PS composites was studied and models were developed for that system.[36] The behavior of PS-CO_2 system has been modeled by Chiou et al.[43] and by Wissinger and Paulaitis.[44] Wissinger and Paulaitis showed that the T_g of PS decreased to room temperature at a CO_2 pressure of about 60 atmospheres. Condo et al.[45] have also developed a model of this phenomenon for amorphous polymers based on lattice free energy, applying it to PMMA-CO_2 and PS-CO_2 systems. A T_g of 100°C has been reported for unsaturated PS in various references (for example, see Van Krevelen,[46] Rodriguez,[47] and Billmeyer[48]). Since foaming was conducted at temperatures of 105°C (T_g + 5), 110°C (T_g + 10) and 120°C (T_g + 20), the T_g depression would favor the foaming process. The experimental results of this work clearly showed this issue. In other words, the depression of T_g by dissolved CO_2 enhances foaming at temperatures slightly higher than the T_g of the unsaturated polymer.

Effect of foaming temperature

Scanning electron micrographs of EPS produced at two different temperatures are shown in Figure 6. In the experiment the saturation pressure and foaming times were kept constant at 4.5 MPa and 20 s and the foaming temperature was increased from 105 to 120°C. When the cells are first formed they are discrete and almost spheres, surrounded by thick walls (Fig. 6a). As more gas diffuses into the cells, the expansion continues and the cell walls become thinner and a structure consisting of such a polygonal cells develops (Fig. 6b). Figure 7 schematically represents the steps in development of polygonal structure. Similar observations were made on microcellular foaming of polysolfunes.[49]

Diffusion of CO_2 gas from the polymer into cells is a controlling parameter for cell size. When the foaming time increases, more gas can diffuse into the cells, which leads to the production of larger cell sizes.

The viscosity of polymer decreased with increasing temperature, facilitating cell growth. An increase of diffusivity of gas within the polymer is another factor producing larger cell sizes at higher temperature.

Effect of foaming time

Figure 8 shows the microstructures of EPS produced at two different foaming times. The cell density and

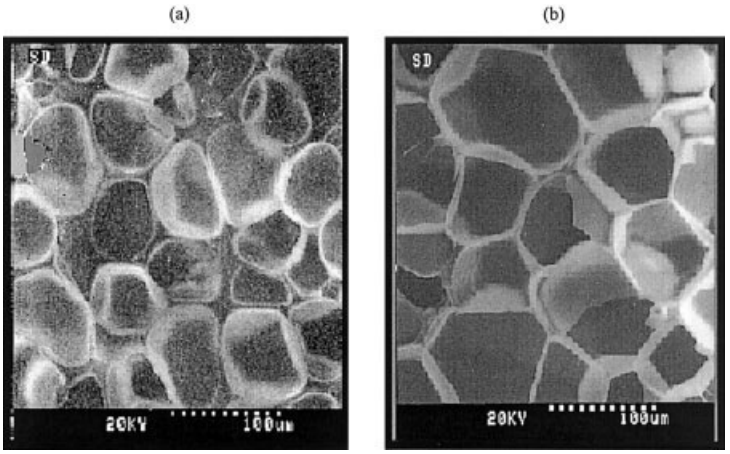

Figure 6 SEM micrographs of the specimens produced at foaming temperatures (a) 105°C and (b) 120°C. $P = 4.5$ MPa and $t = 20$ s.

cell size increased when the foaming time increased from 10 to 30 s. For these experiments saturation pressure and foaming temperature were set at 4.5 MPa and 110°C. Interestingly, the cell size was more sensitive to the foaming time (the plot has a larger slope) at lower saturation pressures (see Fig. 2), while cell density was more sensitive to foaming time at higher saturation pressures (see Fig. 3). The cell density decreased with increasing foaming time, but the effect of foaming time on cell size became less significant as the saturation pressure increased. Earlier, it was stated that the number of nucleated bubbles strongly depends on the saturation pressure. An increase in saturation pressure decreases the free energy of nucleation and eventually exponentially increases the number of nuclei.

When foaming time increased, more gas molecules diffused from the polymer matrix into the cells during expansion, and hence the density was decreased. Statistical analysis identified foaming time as the most important parameter controlling foam density, which means that the kinetics of desorption are paramount in this process. This is not unexpected since the sorption time was 20 h (at room T), and only a matter of tens of seconds (at the foaming T) were allowed for foaming prior to quenching.

The time-temperature equivalence principle can be used to explain the effect of foaming temperature. In general, a change in temperature has a significant effect on the physical properties of polymers. This applies particularly to the viscoelastic properties. According to the time-temperature equivalence principle, an increase in temperature accelerates molecular motions and decreases the viscosity and polymer chain stiffness. This phenomenon brings the system more rapidly to equilibrium, accelerating all types of viscoelastic processes.[45] Williams et al.[50] explained this phenomenon and proposed an expression for the effect of temperature and time on the viscoelastic behavior of polymers. Time and temperature influence viscoelasticity through the product of actual time and a factor a_T, which is called the shift factor, and is related to the free volume. Williams et al. proposed the following equation:

$$\log a_T = [-13.3(T - T_g)]/(47.5 + T - T_g) \qquad (8)$$

This equation is found to be valid at temperatures between T_g and T_g + 100°C. The factor a_T represents the horizontal shift of stress-relaxation master curves along time axis to the reference temperature when the temperature or time changes. Actually, a_T relates the

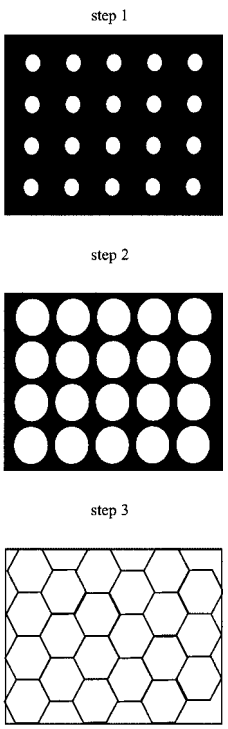

Figure 7 Development of polygonal structure in EPS.

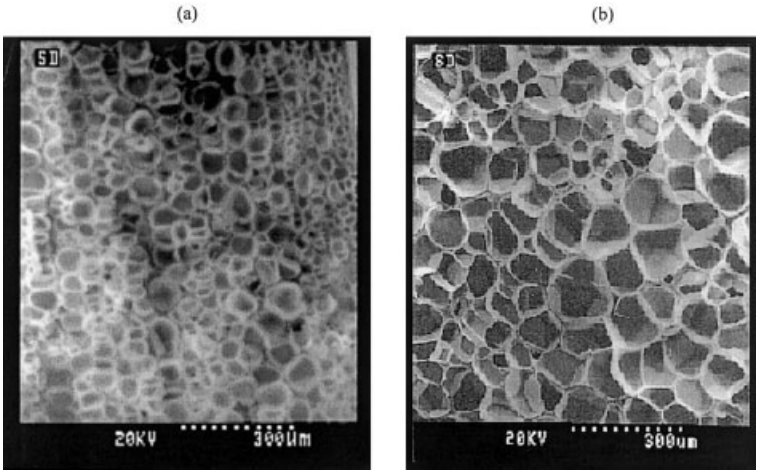

Figure 8 SEM micrographs of the specimens produced at foaming times (a) 10 s and (b) 30 s. $P = 4.5$ MPa and $T = 110$°C.

effects of time and temperature on the viscoelastic properties of polymers. In other words, the same effect is obtained when the time or temperature is changed.

Relationship between cell size, cell density, and foam density

The goal of this study was to control microstructure of EPS by controlling the process parameters. The plot of cell size versus foam density (Fig. 9) indicates that by controlling the foaming conditions one can produce foams having the same density and different cell sizes and cell densities. For example, foams produced at 4.5 MPa, 120°C and 20 s and at 3 MPa, 120°C and 30 s exhibited the same foam relative densities of 0.128, but had average cell sizes of 133 and 341 μm, respectively. In order to conduct a systematic investigation of the effect of cell size and foam density on the properties of the expanded polymer it is very important to be able to produce foam specimens with controlled density and cell size in this way.

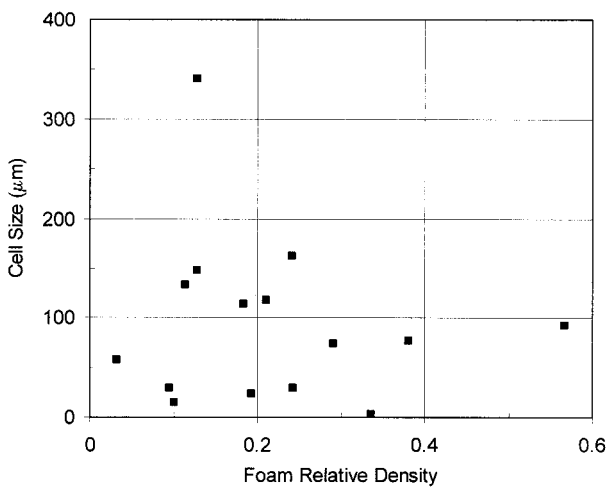

Figure 9 Correlation between cell size and foam relative density for samples produced under different conditions.

CONCLUSIONS

The effects of foaming conditions of PS on the structure of the resulting foams were investigated. By controlling the foaming conditions, including saturation pressure, foaming temperature, and foaming time, a wide range of foam densities and cell sizes can be produced. The results of the statistical analysis of the model terms showed that foaming time was the most important factor determining foam density, followed by foaming temperature and saturation pressure. Moreover, saturation pressure was the most important factor controlling cell size and cell density, followed by foaming time and foaming temperature. It was observed that by controlling the foaming conditions, foams having the same densities and different cell sizes and cell densities could be produced. The foams produced with controlled structures were used in the next part to study the structure-property relationship. In continuing this work the range of obtained structures can be extended more by using supercritical CO_2.

The authors gratefully acknowledge partial funding for this research provided by the University of Toronto. Thanks also to Nova Chemicals (Calgary, Canada) for providing materials and to Mr. Shiang Law for technical assistance.

References

1. Klempner, D.; Fritsch, K. C. Handbook of polymeric foams and foam technology; Hanser Publishers: Munich, 1991.
2. Seeler, K. A.; Kumar, V. SPE ANTEC Tech Papers 1992, 38, 1503.
3. Collias, D. I.; Baird, D. G.; Borggreve, R. J. M. Polymer 1994, 35, 3978.
4. Pfleummer, F. Ger. Pat. 249,777 (1920).

5. Alderson, W. L. U.S. Pat. 2,387,730 (1945).
6. Gent, A. N.; Tompkins, D. A. J Appl Phys 1969, 40, 2520.
7. Hendrey, J. W.; U.S. Pat. 3,962,387 (1976).
8. Martini, J. E.; Waldman, F. A.; Suh, N. P. SPE ANTEC Tech Papers 1982, 28, 674.
9. Martini-Vvedensky, J. E.; Suh, N. P.; Waldman, F. A. U.S. Pat. 4,473,665 (1984).
10. Arora, K. A.; Lesser, A. J.; McCarthy, T. J. Macromolecules 1998, 31, 775.
11. Sumarno; Sato, Y.; Takishima, S; Masuoka, H. J App Polym Sci, 2000, 77, 2383.
12. Dixon, D. J.; Lyna-Barcenas, G.; Johnston, K. P. Polymer 1994, 18, 3998.
13. Aubert, J. H.; Clough, R. L. Polymer 1985, 26, 2047.
14. Lloyd, D. R.; Kim, S. S.; Kinzer K. E. J Membrane Sci 1991, 64, 1.
15. Tsai, F.; Torkelson, J. M. Macromolecules 1990, 23, 775.
16. Pinnau, I. Ph.D. Thesis, University of Texas at Austin, 1991.
17. Smolders, C. A. Proceeding Of the Symposium on Ultrafiltration Membranes and Applications; Plenum Press: New York, 1980.
18. Kawashima, Y.; Niwa, T.; Takeuchi, H.; Hino, T.; Ito, Y. J Controlled Release 1991, 16, 279.
19. Bodmeier, R.; Chen, H. J. J Pharm Pharmacol 1988, 40, 745.
20. Nauman, E. B.; Ariapadi, M. V.; Balsara, N. P.; Grocela, T. A.; Liu, J. S.; Mallikarjun, R. Chem Eng Commun 1988, 66, 29.
21. Matson, D. W.; Fulton, J. L.; Petersen, R. C.; Smith, R. D. Ind Eng Chem Res 1987, 26, 2298.
22. Tom, J. W.; Debenedetti, P. G. J Aerosol Sci 1991, 22, 555.
23. Lele, A. K.; Shine, A. D. AIChE J 1992, 38, 742.
24. Pekala, R. W. J Mater Sci 1988, 24, 3221.
25. Srinivasan, G.; Elliott, Jr. Ind Eng Chem Res 1992, 31, 1414.
26. Kumar, V.; Suh, N. P. Polym Eng Sci 1990, 30, 1323.
27. Kumar, V.; Schirmer, G. SPE ANTEC Tech Papers 1995, 41, 2189.
28. Baldwin, D. F.; Park, C. B.; Suh, N. P. Polym Eng Sci 1996, 36, 1425.
29. Park, C. B.; Suh, N. P. Polym Eng Sci 1996, 36, 34.
30. Behravesh, A. H.; Park, C. B.; Venter, R. D. ASME Cellular and microcellular materials 1996, 76, 47.
31. Khemani, K. C. In Polymeric Foams: Science and Technology; Khemani, K. C., Ed.; ACS Symposium Series, 1997, 669, 54.
32. Dey, S. K.; Natarajan, P.; Xanthos, M. SPE ANTEC Tech Papers 1996, 42, 2042.
33. Klotzer, R.; Paul, D.; Seilbig, B. SPE ANTEC Tech Papers 1997, 43, 1955.
34. Siripuraru, S.; Gay, Y. J.; Royer, J. P.; DeSimone, J. M.; Khan, S. A.; Spontak, R. J., Mat Res Soc Symp 2000, 626, FF9.9.1.
35. Shimoda, M.; Tanigaki, M.; Ohshima, M.; Tsujimura, I. J Cell Plastics, 2001, 37, 517.
36. Doroudiani, S.; Chaffey, C. E.; Kortschot, M. T. J Polym Sci Part B: Polym Phys 2002, 40, 723.
37. Doroudiani, S. Ph.D. Thesis, Department of Chemical Engineering and Applied Chemistry, University of Toronto, 1998.
38. Verseput. Designed Experiments and Information, S-Matrix, USA 1995.
39. Montgomery, D.C. Design and analysis of experiments, 4th ed.; Wily: New York, 1997.
40. Kumar, V.; Weller, J. E. ASME, Cell Microcell Mater, 1996, 76, 17.
41. Lubetkin, S. D. In Controlled Particle, Droplet, Bubble Formation; Wedlock, D. J., Ed.; Butterworth-Heinemann Ltd: Woburn, MA, 1994.
42. Assink, R. A. J Polym Sci 1974, 12, 2281.
43. Chiou, J. S.; Barlow, J. W.; Paul, D. R. J Appl Polym Sci 1985, 30, 2633.
44. Wisinger, R. G.; Paulaitis, M. E. J Polym Sci Part B: Polym Phys 1991, 29, 631.
45. Condo, P. D.; Isanchez, C.; Panayiotou, C. G.; Johnston, K. P. Macromolecules 1992, 25, 6119.
46. Van Krevelen; D. W. Properties of Polymers, 3rd ed.; Elsevier Science: Amsterdam, 1990.
47. Rodriguez, F. Principles of Polymer Systems, 2nd ed.; McGraw-Hill: New York, 1985.
48. Billmeyer, F. W. Textbook of Polymer Science, 3rd ed.; Wiley-Interscience: New York, 1984.
49. Sun, H.; Sur, G. S.; Mark, J. E. Eur Polym J 2002, 38, 2373.
50. Williams, M. L.; Landel, R. F.; Ferry, I. D. J Am Chem Soc 1955, 77, 3701.